Weierstraß-Institut
für Angewandte Analysis und Stochastik
Leibniz-Institut im Forschungsverbund Berlin e. V.

Preprint ISSN 2198-5855

Numerical approach to a model for quasistatic damage with spatial BV-regularization

Sören Bartels[1], Marijo Milicevic[1], Marita Thomas[2]

submitted: April 19, 2017 (revision: October 9, 2017)

[1] Department of Applied Mathematics
Mathematical Institute
University of Freiburg
Hermann-Herder-Str. 9
79104 Freiburg i. Br.
Germany
E-Mail: bartels@mathematik.uni-freiburg.de
marijo.milicevic@mathematik.uni-freiburg.de

[2] Weierstrass Institute
Mohrenstr. 39
10117 Berlin
Germany
E-Mail: marita.thomas@wias-berlin.de

No. 2388
Berlin 2017

2010 *Mathematics Subject Classification.* 35K85, 74R05, 49J45, 49S05, 65M12.

Key words and phrases. Partial damage, damage evolution with spatial regularization, functions of bounded variation, semistable energetic solutions, numerical approximation.

This work was carried out within the project *Finite element approximation of functions of bounded variation and application to models of damage, fracture, and plasticity* within the DFG Priority Programme SPP 1748 "Reliable Simulation Techniques in Solid Mechanics. Development of Non-standard Discretisation Methods, Mechanical and Mathematical Analysis."

Edited by
Weierstraß-Institut für Angewandte Analysis und Stochastik (WIAS)
Leibniz-Institut im Forschungsverbund Berlin e. V.
Mohrenstraße 39
10117 Berlin
Germany

Fax: +49 30 20372-303
E-Mail: preprint@wias-berlin.de
World Wide Web: http://www.wias-berlin.de/

Numerical approach to a model for quasistatic damage with spatial BV-regularization

Sören Bartels, Marijo Milicevic, Marita Thomas

Abstract

We address a model for rate-independent, partial, isotropic damage in quasistatic small strain linear elasticity, featuring a damage variable with spatial BV-regularization. Discrete solutions are obtained using an alternate time-discrete scheme and the *Variable*-ADMM algorithm to solve the constrained nonsmooth optimization problem that determines the damage variable at each time step. We prove stability of the method and show that a discrete version of a semistable energetic formulation of the rate-independent system holds. Moreover, we present our numerical results for two benchmark problems.

1 The damage model, its solution concept, and our results

By damage evolution we understand the formation and growth of cracks and voids in the microstructure of a solid material. This process is monitored over a time interval $[0,\mathsf{T}]$ for a body with reference configuration $\Omega \subset \mathbb{R}^d$, $d > 1$. In the spirit of generalized standard materials [27] and continuum damage mechanics [32, 33] this degradation phenomenon is modeled by a volumetric internal damage variable $z : [0,\mathsf{T}] \times \Omega \to [0,1]$ which is incorporated into the constitutive law in order to reflect the changes of the elastic behavior due to damage. It is assumed that the length scale of the specimen of the considered material is much larger than that of the respective *reference volume*. The reference volume of a material is a characteristic volume such that all relevant properties of the material are comprised in this amount of material and such that the material can be regarded as homogeneous if it is considered in a much larger length scale than the length scale of the reference volume. The value $z(t,x)$ at $(t,x) \in [0,\mathsf{T}] \times \Omega$ can then be understood as the undamaged fraction of the reference volume at time t located in $x \in \Omega$.

The evolution of the damage variable is driven by time-dependent external loads, which cause the deformation of the body and increase its stresses. To relax, damage evolves and thus turns stored energy into dissipated energy. These two energy contributions can be described by an energy functional $\mathscr{E}$ and a dissipation potential $\mathscr{R}$. In literature many different assumptions have been made with regard to the growth properties of the two functionals, which directly affect the regularity properties of the damage variable with regard to time and space. In this way the contributions to damage processes in mathematical and engineering literature can be divided into two major classes: One class considers the evolution of damage as a rate-dependent phaenomenon, mostly modeled by a viscous dissipation with quadratic growth, cf., e.g., [18, 17, 29, 7, 8, 47], and a further class understands damage as a rate-independent process described by a positively 1-homogeneous dissipation potential, cf., e.g., [28, 35, 11, 15, 43, 56, 54, 55]. While the first growth property leads comparably smooth evolution in time settled in $L^2(\Omega)$, the latter only provides bounded variations in time, so that the damage variable may jump in time. Indeed, the use of a rate-independent model, resp. the neglection of rate-effects, is also seen as a feasible approximation for certain damage processes observed in experiments, cf., e.g.,

DOI 10.20347/WIAS.PREPRINT.2388

[25]. We will follow the latter concept and consider the positively 1-homogeneous dissipation potential $\mathscr{R} : \mathbf{Z} \to \mathbb{R} \cup \{\infty\}$,

$$\mathscr{R}(v) := \int_\Omega \mathrm{R}(v)\,\mathrm{d}x, \quad \text{with } \mathrm{R}(v) := \begin{cases} \rho|v|\,\mathrm{d}x & \text{if } v \in (-\infty, 0], \\ +\infty & \text{if } v > 0 \end{cases} \tag{1a}$$

$$\text{with } \mathbf{Z} := L^1(\Omega), \tag{1b}$$

and with a constant dissipation rate $\rho > 0$. Due to the convention $z = 1$ for the unbroken and $z = 0$ for the broken state of the material, the dissipation potential ensures the unidirectionality of the process and thus prevents healing of the material.

Also for the energy functional $\mathscr{E}$ different regularity assumptions have been made for the damage variable: By now, it has become a well-accepted approach to incorporate damage gradients into the energy, in order to account for nonlocal effects of damage from a physical point of view, and to benefit from its regularizing effect in the mathematical analysis and numerical simulations. The vast majority of contributions considers a damage gradient with growth of power $p = 2$ [18, 17, 26, 7, 8, 40, 38, 57, 53, 2, 37, 34]. For technical reasons, sometimes also $p > d$ is chosen, cf., e.g., [42, 29, 47]. It has to be remarked that this choice has direct influence on the effects of damage that can be observed with this model: For gradient regularizations of this type, mathematically, the damage variable is an element in a Sobolev space, and transitions between damaged and undamaged material phases have to be smooth and thus have to take place in zones of a certain positive width. The assumption $p > d$ enforces that the damage variable even has to be continuous in space. Yet, from own experience one can also observe situations where the transition between damaged and undamaged regions is very sharp. This effect cannot be described by a regularization in Sobolev spaces. Therefore it is the aim of this work to contribute to the toolbox for the investigation of damage processes with a model that allows for sharp transitions between damaged and undamaged material phases. To capture this effect, but still to benefit from regularizing effects of gradients, we propose to replace the Sobolev-gradient by a BV-gradient. More precisely, we shall consider the function spaces

$$\mathbf{U} := \{v \in H^1(\Omega, \mathbb{R}^d),\, v = 0 \text{ on } \Gamma_D \text{ in trace sense}\}, \tag{2a}$$

$$\mathbf{X} := BV(\Omega), \tag{2b}$$

and an energy functional $\widehat{\mathscr{E}} : [0, \mathrm{T}] \times \mathbf{U} \times \mathbf{X} \to \mathbb{R} \cup \{\infty\}$ of the form

$$\begin{aligned} \widehat{\mathscr{E}}(t,u,z) := \frac{1}{2} \int_\Omega f(z)\big(\lambda \big|\operatorname{tr} e(u+g(t))\big|^2 + 2\mu|e(u+g(t))|^2\big)\,\mathrm{d}x \\ + \kappa|\mathrm{D}z|(\Omega) + \int_\Omega I_{[0,1]}(z)\,\mathrm{d}x - \int_{\Gamma_{\mathrm{Neu}}} u_{\mathrm{Neu}}(t) \cdot (u+g(t))\,\mathrm{d}s \end{aligned} \tag{3}$$

with the Lamé constants $\lambda, \mu > 0$, $e(u) := \frac{1}{2}(\nabla u + \nabla u^\top)$ the linear-strain tensor, $g : [0, \mathrm{T}] \times \Omega \to \mathbb{R}^d$ a suitable extension of a given Dirichlet datum into the domain Ω and $u_{\mathrm{Neu}} : [0, \mathrm{T}] \times \Gamma_{\mathrm{Neu}} \to \mathbb{R}^d$ a given surface loading acting along the Neumann-boundary Γ_{Neu}. Due to the mapping properties of the monotonously increasing function $f : [0,1] \to [a,b]$ with constants $0 < a < b$ the model will capture partial damage only: It is $f(0) \geq a$ and hence, even in the state of maximal damage the solid has the ability to counteract external loadings with suitable stresses and displacements; for models allowing for complete damage, where this property is lost, we refer, e.g., to [9, 44, 30]. The compactness information needed to handle the product of $f(z)$ and quadratic terms in e is provided by the total variation $|\mathrm{D}z|(\Omega)$ of z in Ω, weigthed with a constant $\kappa > 0$,. Finally, the indicator function $I_{[0,1]}$

confines the values of z to the interval $[0,1]$, i.e., $I_{[0,1]}(z)=0$ if $z\in[0,1]$ and $I_{[0,1]}(z)=\infty$ otherwise. In view of (1b), we will work with the extended energy functional $\mathscr{E}:[0,\mathsf{T}]\times\mathbf{U}\times\mathbf{Z}\to\mathbb{R}\cup\{\infty\}$

$$\mathscr{E}(t,u,z):=\begin{cases}\widehat{\mathscr{E}}(t,u,z) & \text{if } (u,z)\in\mathbf{U}\times\mathbf{X},\\ \infty & \text{otherwise.}\end{cases} \tag{4}$$

It is the aim of this paper to study the existence of solutions for the rate-independent system $(\mathbf{U}\times\mathbf{Z},\mathscr{E},\mathscr{R})$ given by (2), (4), (1a) by proving the convergence of a numerical method. For this, we will impose a partition $\Pi_N:=\{t_N^k,\,k\in\{0,1,\ldots,N\},0=t_N^0<\ldots<t_N^N=\mathsf{T}\}$ of the time-interval $[0,\mathsf{T}]$ and a space discretization in terms of $P1$ finite elements, yielding finite-element spaces $\mathbf{U}_h,\mathbf{X}_h$. At each time-step $t_N^k\in\Pi_N$, we will determine approximate solutions in $\mathbf{U}_h,\mathbf{X}_h$ via an alternating minimization scheme, i.e., starting from an approximation $(u_{0h},z_{0h})\in\mathbf{U}_h\times\mathbf{X}_h$ of the initial datum (u_0,z_0) at t_N^0, we alternatingly compute for given $(u_{Nh}^0,z_{Nh}^0)=(u_{0h},z_{0h})$

$$u_{Nh}^k=\operatorname{argmin}_{u\in\mathbf{U}_h}\mathscr{E}(t_k,u,z_{Nh}^{k-1}), \tag{5a}$$

$$z_{Nh}^k\in\operatorname{argmin}_{z\in\mathbf{X}_h}\mathscr{E}(t_k,u_{Nh}^k,z)+\mathscr{R}(z-z_{Nh}^{k-1}). \tag{5b}$$

While the computation of u_{Nh}^k reduces to the solution of a linear system of equations, the computation of z_{Nh}^k requires the solution of a constrained nonsmooth minimization problem. This problem is qualitatively of the form of the Rudin-Osher-Fatemi (ROF) problem [52] for which various numerical schemes have been proposed for its iterative solution, cf., e.g., [3, 6, 13, 14, 23, 24, 31, 36, 48, 59]. We approximate a minimizer z_{Nh}^k by converting the minimization problem into a saddle-point problem and use a variant of the alternate direction method of multipliers (ADMM) [16, 19, 20, 21, 22] recently introduced in [5] as *Variable-ADMM* for the approximate solution of the saddle-point problem.

We show stability of the alternate minimization scheme and prove that suitable interpolants constructed from (5) satisfy a discrete version of a semistable energetic formulation of the system $(\mathbf{U}\times\mathbf{Z},\mathscr{E},\mathscr{R})$:

Definition 1.1 (semistable energetic solution) *A function $q=(u,z):[0,\mathsf{T}]\to\mathbf{U}\times\mathbf{Z}$ is called semistable energetic solution for the system $(\mathbf{U}\times\mathbf{Z},\mathscr{E},\mathscr{R})$, if $t\to\partial_t\mathscr{E}(t,q)\in L^1((0,\mathsf{T}))$ and if for all $s,t\in[0,\mathsf{T}]$ we have $\mathscr{E}(t,q(t))<\infty$, if for a.a. $t\in(0,\mathsf{T})$ minimality condition* (6a) *is satisfied and if for all $t\in[0,\mathsf{T}]$ semistability* (6b) *as well as the upper energy-dissipation estimate* (6c) *hold true, i.e.:*

$$\text{for all } \tilde{u}\in\mathbf{U}:\quad \mathscr{E}(t,u(t),z(t))\leq\mathscr{E}(t,\tilde{u},z(t)), \tag{6a}$$

$$\text{for all } \tilde{z}\in\mathbf{X}:\quad \mathscr{E}(t,u(t),z(t))\leq\mathscr{E}(t,u(t),\tilde{z})+\mathscr{R}(\tilde{z}-z(t)), \tag{6b}$$

$$\mathscr{E}(t,q(t))+\mathscr{R}(z(t)-z(0))\leq\mathscr{E}(0,q(0))+\int_0^t\partial_\xi\mathscr{E}(\xi,q(\xi))\,\mathrm{d}\xi\,, \tag{6c}$$

where the dissipated energy up to time t is given by the total variation induced by the dissipation potential $\mathscr{R}$ with unidirectionality constraint and, by the induced monotonicity of $z:[0,\mathsf{T}]\to\mathbf{Z}$, takes the form $\mathscr{R}(z(t)-z(0))$.

Let us note here that the alternate minimization scheme (5) directly leads to the notion of semistable energetic solutions. In the quasistatic, rate-independent setting they form a much wider class than the well-known energetic solutions, cf., e.g., [41, 43], which replace conditions (6a) & (6b) by the joint global stability condition $\forall(\tilde{u},\tilde{z})\in\mathbf{U}\times\mathbf{Z}:\mathscr{E}(t,u(t),z(t))\leq\mathscr{E}(t,\tilde{u},\tilde{z})+\mathscr{R}(\tilde{z}-z(t))$ and the upper energy-dissipation estimate (6c) by an energy-dissipation *balance*. In fact, the existence of energetic solutions for the above system $(\mathbf{U}\times\mathbf{Z},\mathscr{E},\mathscr{R})$ was investigated in [54]. As a matter of concept, energetic solutions are obtained from a time-discrete scheme with a monolithic minimization in the pair

(u,z) in each time step. In the case that $\mathscr{E}(t,\cdot,\cdot)$ is jointly convex in the pair (u,z) it can be shown that semistable energetic solutions are also energetic solutions. However, this is not true if the energy functional does not enjoy the property of joint convexity. In this case it can be observed that energetic solutions tend to evolve earlier than semistable energetic solutions, cf., e.g., [49]. Indeed, many energy functionals taken from engineering literature are separately convex in the variables u and z but not jointly convex, cf. [56, Sec. 5] for examples on convexity properties of damage models.

Our paper is organized as follows: In Section 2 we state the main assumptions needed for the analysis. Section 3 introduces the numerical algorithms used to calculate approximate solutions in the sense of (5). We present the Variable-ADMM adjusted to the present setting, address its stability and the monotonicity of the residual and prove that the residual controls the difference between the optimal energy and the energy of the iterates. Based on this, in Section 4 we prove the stability of the fully discretized problem. We also show that the solutions satisfy a discrete version of the semistable energetic formulation as well as uniform apriori estimates. This is the basis for the limit passage to the notion of solution given in Definition 1.1, which, however, we do not carry out in this work. Finally, in Section 5 we report our numerical results for an academic example and a benchmark problem from engineering.

2 Setup and notation

Throughout this work, we consider the time interval $[0,\mathsf{T}]$ for some time horizon $\mathsf{T}>0$ and an open bounded Lipschitz domain $\Omega\subset\mathbb{R}^d$, $d=2,3$, with Dirichlet boundary $\Gamma_D\subset\partial\Omega$ with $(d-1)$-dimensional Hausdorff-measure $\mathscr{H}^{d-1}(\Gamma_D)>0$. We denote by $(\cdot,\cdot)$ the L^2-inner product, by $\|\cdot\|$ the L^2-norm, and by $|\cdot|$ the Euclidean norm on $\mathbb{R}^d$. Moreover, by $\mathrm{B}([0,\mathsf{T}],\bullet)$ we denote the space of functions f mapping time into a space $\bullet$, which are bounded and defined everywhere in $[0,\mathsf{T}]$.

Regarding the given data appearing in (3) we make the following assumptions:

Assumption 2.1 (Assumptions on the given data) *1 The function $f:\mathbb{R}\to\mathbb{R}$ is continuously differentiable and convex and such that $f|_{[0,1]}:[0,1]\to[a,b]$ is monotonically increasing.*

2 The Lamé constants satisfy $\lambda,\mu>0$.

3 The extension of the Dirichlet datum is of regularity $g\in C^1([0,\mathsf{T}],H^1(\Omega;\mathbb{R}^d))$ with $C_g:=\|g\|_{C^1([0,\mathsf{T}],H^1(\Omega;\mathbb{R}^d))}$.

4 The Neumann datum u_{Neu} is of regularity $u_{\mathrm{Neu}}\in C^1([0,\mathsf{T}],L^2(\Gamma_{\mathrm{Neu}};\mathbb{R}^d))$ with $C_{u_{\mathrm{Neu}}}:=\|u_{\mathrm{Neu}}\|_{C^1([0,\mathsf{T}],L^2(\Gamma_{\mathrm{Neu}};\mathbb{R}^d))}$

Moreover, for the space discretization we will use the following notation related to **finite element spaces**: Let $(\mathscr{T}_h)_{h>0}$ be a family of triangulations of Ω where the index h denotes the mesh size $h=\max_{T\in\mathscr{T}_h}h_T$ with h_T being the diameter of the simplex T. The minimal diameter is given by $h_{\min}=\min_{T\in\mathscr{T}_h}h_T$. The sets $\mathscr{N}_h$ and E_h contain all nodes and edges, respectively, of the triangulation $\mathscr{T}_h$. We will use the finite element space of continuous, piecewise affine functions ($r=1$) or vector fields ($r=d$), denoted by $\mathscr{S}^1(\mathscr{T}_h)^r$ and of elementwise constant vector fields $\mathscr{L}^0(\mathscr{T}_h)^d$, i.e.,

$$\mathscr{S}^1(\mathscr{T}_h)^r := \{v_h\in C(\Omega;\mathbb{R}^r):\ v_h|_T \text{ affine for all } T\in\mathscr{T}_h\}, \tag{7a}$$

$$\mathscr{L}^0(\mathscr{T}_h)^d := \{\tilde{p}_h\in L^\infty(\Omega;\mathbb{R}^d):\ \tilde{p}_h|_T \text{ constant for all } T\in\mathscr{T}_h\}. \tag{7b}$$

Moreover, denoting by $\mathscr{I}_h: C^0(\overline{\Omega})\to\mathscr{S}^1(\mathscr{T}_h)$ the standard nodal interpolation operator we will consider the discrete inner products

$$(v_h, w_h)_h := \int_\Omega \mathscr{I}_h[v_h w_h]\,\mathrm{d}x = \sum_{y\in\mathscr{N}_h} \beta_y v_h(y) w_h(y) \quad \text{on } \mathscr{S}^1(\mathscr{T}_h),$$

$$(p_h, \tilde p_h)_w := h_{\min}^d (p_h, \tilde p_h) \quad \text{on } \mathscr{L}^0(\mathscr{T}_h)^d,$$

where $\beta_y = \int_\Omega \varphi_y\,\mathrm{d}x$ with φ_y the nodal basis function associated to $y \in \mathscr{N}_h$. We have the relations

$$\|v_h\| \le \|v_h\|_h \le (d+2)^{1/2}\|v_h\|, \quad \text{and} \quad \|\tilde p_h\|_w \le c\|\tilde p_h\|_{L^1(\Omega)},$$

for all $v_h \in \mathscr{S}^1(\mathscr{T}_h)$ and $\tilde p_h \in \mathscr{L}^0(\mathscr{T}_h)^d$, see [4, Lemma 3.9] and [12, Thm. 4.5.11]. Finally, for a sequence of step sizes $(\tau_j)_{j\in\mathbb{N}}$ and functions $(a^j)_{j\in\mathbb{N}}$ we will denote the backward difference quotient by

$$d_t a^j = \frac{a^j - a^{j-1}}{\tau_j}.$$

3 Numerical Method

We now discuss the numerical algorithms used to solve the alternate minimization problem (5) on the discrete level. With $\mathscr{S}^1(\mathscr{T}_h)^d$ and $\mathscr{S}^1(\mathscr{T}_h)$ from (7) we set $\mathbf{U}_h := \mathscr{S}^1(\mathscr{T}_h)^d \cap \{v \in C(\overline{\Omega};\mathbb{R}^d), v = 0 \text{ on } \Gamma_D\} \subset H_D^1(\Omega;\mathbb{R}^d)$ in (5a) and $\mathbf{X}_h := \mathscr{S}^1(\mathscr{T}_h) \subset BV(\Omega)$ in (5b). While the minimization problem (5a) to determine u_{Nh}^k reduces to the solution of a linear system of equations, the minimization problem (5b) to find z_{Nh}^k is more difficult due to the non-differentiability of the BV-seminorm and the occurence of non-smooth constraints in $\mathscr{E}$ and $\mathscr{R}$. We will deal with the minimization problem (5b) in Subsection 3.1 and subsequently explain the algorithm for the full alternate minimization problem in Subsection 3.2.

3.1 Minimization with respect to z in (5b)

For the following discussion we consider a partition Π_N of $[0,\mathsf{T}]$ with $N \in \mathbb{N}$ fixed. We also keep $t_N^k \in \Pi_N$ and u_{Nh}^k the solution of (5a) fixed. For simpler notation we here write $t_k = t_N^k$, $u_h^k = u_{Nh}^k$, and $z_h^k = z_{Nh}^k$, i.e., we do not indicate the dependence of these quantities on $N \in \mathbb{N}$ fixed. We first of all note that a minimizer $z_h^k = z_{Nh}^k$ obtained in (5b) is required to satisfy $z_h^k - z_h^{k-1} \le 0$ almost everywhere in Ω since otherwise $\mathscr{R}(z_h^k - z_h^{k-1})$ is infinite. Since $z_h^k, z_h^{k-1} \in \mathbf{X}_h = \mathscr{S}^1(\mathscr{T}_h)$ are globally continuous and piecewise affine this is equivalent to $z_h^k(x) \le z_h^{k-1}(x)$ for all $x \in \mathscr{N}_h$. Particularly, $|z_h^k(x) - z_h^{k-1}(x)| = z_h^{k-1}(x) - z_h^k(x)$. Hence, letting for $k \ge 1$

$$K_k := \{v_h \in \mathscr{S}^1(\mathscr{T}_h) :\ 0 \le v_h(x) \le z_h^{k-1}(x)\ \forall\, x \in \mathscr{N}_h\} \tag{8}$$

we define the auxiliary functional $\widetilde{\mathscr{E}}(t_k,\cdot,\cdot) : \mathbf{U}_h \times \mathbf{X}_h \to \mathbb{R} \cup \{\infty\}$,

$$\begin{aligned}\widetilde{\mathscr{E}}(t_k, u_h, z_h) := \frac{1}{2}\int_\Omega f(z_h)\big(\lambda|\operatorname{tr} e(u_h + g(t_k))|^2 + 2\mu|e(u_h + g(t_k))|^2\big)\,\mathrm{d}x \\ - \int_{\Gamma_{\mathrm{Neu}}} u_{\mathrm{Neu}}(t_k)\cdot(u_h + g(t_k))\,\mathrm{d}s + \kappa\int_\Omega |\nabla z_h|\,\mathrm{d}x + I_{K_k}(z_h).\end{aligned}$$

We obtain that minimality property (5b) is equivalent to

$$z_h^k \in \operatorname{argmin}_{z_h \in \mathbf{X}_h} \widetilde{\mathscr{E}}(t_k, u_h^k, z_h) - \rho(z_h, 1).$$

In order to approximate a minimizer z_h^k we consider for $\tau_j > 0$ and $\mathbb{C}A = \lambda\,\mathrm{tr}(A)I + 2\mu A$ for $A \in \mathbb{R}^{d\times d}$ the augmented Lagrangian functional

$$\begin{aligned} L_h^k(z_h,p_h,s_h;\eta_h,\zeta_h) := &\frac{1}{2}\int_\Omega f(z_h)e(u_h^k+g(t_k)) : \mathbb{C}e(u_h^k+g(t_k))\,\mathrm{d}x - \rho(z_h,1)\\ &+\kappa\int_\Omega |p_h|\,\mathrm{d}x + (\eta_h,\nabla z_h - p_h)_w + \frac{\tau_j}{2}\|\nabla z_h - p_h\|_w^2\\ &+ I_{K_k}(s_h) + (\zeta_h, z_h - s_h)_h + \frac{\tau_j}{2}\|z_h - s_h\|_h^2. \end{aligned}$$

For the approximation of a minimizer z_h^k we use the following algorithm [5] which generalizes the alternating direction method of multipliers (ADMM) established and analyzed, e.g., in [16, 19, 20, 21, 22] by using variable step sizes.

Algorithm 3.1 (Variable-ADMM) *Choose $z_h^0 = z_h^{k-1}$, $\eta_h^0 = 0$ and $\zeta_h^0 = 0$. Choose $\underline{\tau}, \overline{\tau} > 0$ with $\underline{\tau} \le \overline{\tau}$, $\delta \in (0,1)$, $\underline{\gamma}, \overline{\gamma} \in (0,1)$ with $\underline{\gamma} \le \overline{\gamma}$, and $\overline{R} \gg 1$. Set $j = 1$.*
(1) Set $\gamma_1 = \underline{\gamma}$, $\tau_1 = \overline{\tau}$ and $R_0 = \overline{R}$.
(2) Compute a minimizer $(p_h^j, s_h^j) \in \mathscr{L}^0(\mathscr{T}_h)^d \times \mathscr{S}^1(\mathscr{T}_h)$ of

$$(p_h,s_h) \mapsto L_h^k(z_h^{j-1},p_h,s_h;\eta_h^{j-1},\zeta_h^{j-1}).$$

(3) Compute a minimizer $z_h^j \in \mathscr{S}^1(\mathscr{T}_h)$ of

$$z_h \mapsto L_h^k(z_h,p_h^j,s_h^j;\eta_h^{j-1},\zeta_h^{j-1}).$$

(4) Update

$$\begin{aligned} \eta_h^j &= \eta_h^{j-1} + \tau_j(\nabla z_h^j - p_h^j),\\ \zeta_h^j &= \zeta_h^{j-1} + \tau_j(z_h^j - s_h^j). \end{aligned}$$

(5) Define

$$R_j = \left(\|\eta_h^j - \eta_h^{j-1}\|_w^2 + \tau_j^2\|\nabla(z_h^j - z_h^{j-1})\|_w^2 + \|\zeta_h^j - \zeta_h^{j-1}\|_h^2 + \tau_j^2\|z_h^j - z_h^{j-1}\|_h^2\right)^{1/2}.$$

(6) Stop if R_j is sufficiently small.
(7) Define $(\tau_{j+1},\gamma_{j+1})$ as follows:

- *If $R_j \le \gamma_j R_{j-1}$ or if $\tau_j = \underline{\tau}$ and $\gamma_j = \overline{\gamma}$ set*

$$\tau_{j+1} = \tau_j \quad \text{and} \quad \gamma_{j+1} = \gamma_j.$$

- *If $R_j > \gamma_j R_{j-1}$ and $\tau_j > \underline{\tau}$ set*

$$\tau_{j+1} = \max\{\delta\tau_j, \underline{\tau}\} \quad \text{and} \quad \gamma_{j+1} = \gamma_j.$$

- *If $R_j > \gamma_j R_{j-1}$, $\tau_j = \underline{\tau}$ and $\gamma_j < \overline{\gamma}$ set*

$$\tau_{j+1} = \overline{\tau},\ \gamma_{j+1} = \min\left\{\frac{\gamma_j+1}{2}, \overline{\gamma}\right\},\ u^j = u^0 \text{ and } \lambda^j = \lambda^0.$$

(8) Set $j = j+1$ and continue with (2).

In the following proposition we prove that the iterates are bounded, that the algorithm terminates and that the residuals R_j are monotonically decreasing. To this extent we define the functionals

$$F(p_h) = \kappa \int_\Omega |p_h| \,\mathrm{d}x, \quad H(s_h) = I_{K_k}(s_h),$$
$$G(z_h) = \frac{1}{2}\int_\Omega f(z_h) e(u_h^k + g(t_k)) : \mathbb{C} e(u_h^k + g(t_k)) \,\mathrm{d}x - \rho(z_h, 1).$$

Proposition 3.1 (Termination of Alg. 3.1 and monotonicity of residuals) *Let $(z_h, p_h, s_h; \eta_h, \zeta_h)$ be a saddle-point for L_h^k. For the iterates $(z_h^j, p_h^j, s_h^j; \eta_h^j, \zeta_h^j)$, $j \geq 0$, of Algorithm 3.1, the corresponding differences $\delta_\eta^j := \eta_h - \eta_h^j$, $\delta_\zeta^j := \zeta_h - \zeta_h^j$, $\delta_p^j := p_h - p_h^j$, $\delta_s^j := s_h - s_h^j$, and $\delta_z^j := z_h - z_h^j$, and the distance*

$$D_j^2 = \|\delta_\eta^j\|_w^2 + \|\delta_\zeta^j\|_h^2 + \tau_j^2 \|\nabla \delta_z^j\|_w^2 + \tau_j^2 \|\delta_z^j\|_h^2,$$

we have that for every $J \geq 1$ it holds

$$D_J^2 + \sum_{j=1}^{J} R_j^2 \leq D_0^2.$$

In particular, $R_j \to 0$ as $j \to \infty$ and Algorithm 3.1 terminates. Moreover, we have

$$R_{j+1}^2 \leq R_j^2,$$

i.e., the residual is non-increasing.

Proof 3.1 *The optimality conditions for a saddle-point of L_h^k are given by*

$$\begin{aligned} (\eta_h, \tilde{p}_h - p_h)_w + F(p_h) &\leq F(\tilde{p}_h) \quad \forall\, \tilde{p}_h \in \mathscr{L}^0(\mathscr{T}_h)^d, \\ (\zeta_h, r_h - s_h)_h + H(s_h) &\leq H(r_h) \quad \forall\, r_h \in \mathscr{S}^1(\mathscr{T}_h), \\ -(\eta_h, \nabla(w_h - z_h))_w - (\zeta_h, w_h - z_h)_h + G(z_h) &\leq G(w_h) \quad \forall\, w_h \in \mathscr{S}^1(\mathscr{T}_h), \end{aligned} \tag{9}$$

and $p_h = \nabla z_h$ and $s_h = z_h$. On the other hand, with $\widetilde{\eta}_h^j = \eta_h^{j-1} + \tau_j(\nabla z_h^{j-1} - p_h^j)$ and $\widetilde{\zeta}_h^j = \zeta_h^{j-1} + \tau_j(z_h^{j-1} - s_h^j)$, the optimality conditions for the iterates of Algorithm 3.1 read

$$\begin{aligned} (\widetilde{\eta}_h^j, \tilde{p}_h - p_h^j)_w + F(p_h^j) &\leq F(\tilde{p}_h) \quad \forall\, \tilde{p}_h \in \mathscr{L}^0(\mathscr{T}_h)^d, \\ (\widetilde{\zeta}_h^j, r_h - s_h^j)_h + H(s_h^j) &\leq H(r_h) \quad \forall\, r_h \in \mathscr{S}^1(\mathscr{T}_h), \\ -(\eta_h^j, \nabla(w_h - z_h^j))_w - (\zeta_h^j, w_h - z_h^j)_h + G(z_h^j) &\leq G(w_h) \quad \forall\, w_h \in \mathscr{S}^1(\mathscr{T}_h). \end{aligned} \tag{10}$$

Testing (9) and (10) with $(\tilde{p}_h, r_h, w_h) = (p_h^j, s_h^j, z_h^j)$ and $(\tilde{p}_h, r_h, w_h) = (p_h, s_h, z_h)$, respectively, and adding corresponding inequalities gives

$$\begin{aligned} (\widetilde{\eta}_h^j - \eta_h, p_h - p_h^j)_w &\leq 0, \\ (\widetilde{\zeta}_h^j - \zeta_h, s_h - s_h^j)_h &\leq 0, \\ (\eta_h - \eta_h^j, \nabla(z_h - z_h^j))_w + (\zeta_h - \zeta_h^j, z_h - z_h^j)_h &\leq 0. \end{aligned}$$

The rest of the proof of the first estimate is analogous to the proof of [5, Thm. 3.7].

The proof of the monotonicity follows by testing (10) at iterations j and $j+1$ with $(\tilde{p}_h, r_h, w_h) = (p_h^{j+1}, s_h^{j+1}, z_h^{j+1})$ and $(\tilde{p}_h, r_h, w_h) = (p_h^j, s_h^j, z_h^j)$, respectively, and adding the inequalities, which gives

$$\begin{aligned} 0 \leq & -(\widetilde{\eta}_h^{j+1} - \widetilde{\eta}_h^j, p_h^j - p_h^{j+1})_w - (\eta_h^j - \eta_h^{j+1}, \nabla(z_h^j - z_h^{j+1}))_w \\ & - (\widetilde{\zeta}_h^{j+1} - \widetilde{\zeta}_h^j, s_h^j - s_h^{j+1})_h - (\zeta_h^j - \zeta_h^{j+1}, z_h^j - z_h^{j+1})_h. \end{aligned}$$

The monotonicity then follows as in the proof of [5, Prop. 3.11]. ■

In the next step, we show that the residual R_j controls the difference in the objective values.

Lemma 3.1 *Let $(z_h, p_h, s_h; \eta_h, \zeta_h)$ be a saddle-point of L_h^k. Then there exists a constant $C_0 > 0$ such that we have for any $j \geq 1$*

$$\widetilde{\mathscr{E}}(t_k, u_h^k, s_h^j) + \mathscr{R}(s_h^j - z_h^{k-1}) - \widetilde{\mathscr{E}}(t_k, u_h^k, z_h) - \mathscr{R}(z_h - z_h^{k-1}) \leq C_0 R_j. \tag{11}$$

Proof 3.2 *We use the short notation δ_η^j, δ_ζ^j, δ_p^j, δ_s^j and δ_z^j as in Proposition 3.1. Testing (10) with $(\tilde{p}_h, r_h, w_h) = (p_h, s_h, z_h)$, adding the inequalities, noting that $p_h = \nabla z_h$ and $s_h = z_h$ and using $\eta_h^j - \widetilde{\eta}_h^j = \tau_j \nabla(z_h^j - z_h^{j-1})$, $\zeta_h^j - \widetilde{\zeta}_h^j = \tau_j(z_h^j - z_h^{j-1})$ we obtain*

$$\begin{aligned} & F(p_h^j) + G(z_h^j) + H(s_h^j) - F(p_h) - G(z_h) - H(s_h) \\ \leq & -(\widetilde{\eta}_h^j, \delta_p^j)_w + (\eta_h^j, \nabla \delta_z^j)_w - (\widetilde{\zeta}_h^j, \delta_s^j)_h + (\zeta_h^j, \delta_z^j)_h \\ = & -(\eta_h^j, d_t \eta_h^j)_w - \tau_j^2 (\nabla d_t \delta_z^j, \delta_p^j)_w - (\zeta_h^j, d_t \zeta_h^j)_h - \tau_j^2 (d_t \delta_z^j, \delta_s^j)_h. \end{aligned} \tag{12}$$

Testing the optimality conditions of z_h^j and z_h^{j-1} with $w_h = z_h^{j-1}$ and $w_h = z_h^j$, respectively, and adding the corresponding inequalities gives

$$0 \leq -\tau_j^2 (d_t \eta_h^j, \nabla d_t z_h^j)_w - \tau_j^2 (d_t \zeta_h^j, d_t z_h^j)_h.$$

Using $d_t \eta_h^j = \nabla z_h^j - p_h^j$ and $d_t \zeta_h^j = z_h^j - s_h^j$ and inserting $p_h = \nabla z_h$ and $s_h = z_h$ on the right-hand side gives

$$0 \leq -\tau_j^2 (\nabla \delta_z^j, \nabla d_t \delta_z^j)_w + \tau_j^2 (\delta_p^j, \nabla d_t \delta_z^j)_w - \tau_j^2 (\delta_z^j, d_t \delta_z^j)_h + \tau_j^2 (\delta_s^j, d_t \delta_z^j)_h. \tag{13}$$

Adding (12) and (13) we get

$$\begin{aligned} & F(p_h^j) + G(z_h^j) + H(s_h^j) - F(p_h) - G(z_h) - H(s_h) \\ \leq & -(\eta_h^j, d_t \eta_h^j)_w + \tau_j^2 (\nabla \delta_z^j, \nabla d_t z_h^j)_w - (\zeta_h^j, d_t \zeta_h^j)_h + \tau_j^2 (\delta_z^j, d_t z_h^j)_h \\ \leq & \|\eta_h^j\|_w \|d_t \eta_h^j\|_w + \tau_j^2 \|\nabla \delta_z^j\|_w \|\nabla d_t z_h^j\|_w + \|\zeta_h^j\|_h \|d_t \zeta_h^j\|_h + \tau_j^2 \|\delta_z^j\|_h \|d_t z_h^j\|_h \leq C_0 R_j, \end{aligned}$$

with C_0 being bounded due to Proposition 3.1.

Let us furthermore note that by Proposition 3.1 we have that s_h^j and z_h^j are bounded, particularly $0 \leq s_h^j \leq z_h^{k-1}$ for all $j \geq 0$. Since f is Lipschitz continuous on bounded intervals, the Hölder inequality, *the Lipschitz continuity of f and the inverse estimate $\|w_h\|_{L^\infty(\Omega)} \le h^{-d/2}\|w_h\|$ (cf. [12, Thm. 4.5.11]) yield*

$$\frac{1}{2}\int_\Omega (f(s_h^j) - f(z_h^j))e(u_h^k + g(t_k)) : \mathbb{C}e(u_h^k + g(t_k))\,\mathrm{d}x \le ch^{-d/2}\|s_h^j - z_h^j\|.$$

We finally observe that using $s_h^j \le z_h^{k-1}$, $z_h \le z_h^{k-1}$, the triangle inequality, the inverse estimate $\|\nabla w_h\|_{L^1(\Omega)} \le ch^{-1}\|w_h\|_{L^1(\Omega)}$ and the equivalence of $\|\cdot\|$ and $\|\cdot\|_h$ we have

$$\begin{aligned}
&\widetilde{\mathscr{E}}(t_k,u_h^k,s_h^j) + \mathscr{R}(s_h^j - z_h^{k-1}) - \widetilde{\mathscr{E}}(t_k,u_h^k,z_h) - \mathscr{R}(z_h - z_h^{k-1})\\
&= F(p_h^j) + G(z_h^j) + H(s_h^j) - F(p_h) - G(z_h) - H(s_h) + \kappa\int_\Omega \left(|\nabla s_h^j| - |p_h^j|\right)\mathrm{d}x\\
&\quad + \frac{1}{2}\int_\Omega (f(s_h^j) - f(z_h^j))e(u_h^k + g(t_k)) : \mathbb{C}e(u_h^k + g(t_k))\,\mathrm{d}x + \rho\int_\Omega \left(z_h^j - s_h^j\right)\mathrm{d}x\\
&\le C_0R_j + c\kappa h^{-d/2}\|\nabla z_h^j - p_h^j\|_w + c\kappa h^{-1}\|s_h^j - z_h^j\|_h + c(\rho + h^{-d/2})\|z_h^j - s_h^j\|_h\\
&\le C_0R_j.
\end{aligned}$$

which proves the assertion. ■

Remark 3.1 *In general, the iterates $(z_h^j)_{j\ge 0}$ of Algorithm 3.1 may penetrate the obstacles, i.e., $z_h^j \notin K_k$ for some $j \in \mathbb{N}$, cf. (8). Therefore, if $(z_h^{stop}, p_h^{stop}, s_h^{stop}; \eta_h^{stop}, \zeta_h^{stop})$ is the output of the algorithm, we set $z_h^k = s_h^{stop} \in K_k$ to ensure the coercivity of the bulk energy.*

3.2 Alternate minimization (5)

In order to solve the full problem (5) we apply the following scheme:

Algorithm 3.2 (Alternate Minimization) *Choose a stable initial pair $(u_h^0, z_h^0) \in \mathscr{S}^1(\mathscr{T}_h)^d \times \mathscr{S}^1(\mathscr{T}_h)$ and a partition $0 = t = 0 < \ldots < t_N = \mathrm{T}$ of the time interval and set $k = 1$.*
(1) Compute the unique minimizer u_h^k of

$$u_h \mapsto \widetilde{\mathscr{E}}(t_k, u_h, z_h^{k-1}).$$

(2) Compute an approximate minimizer z_h^k of

$$z_h \mapsto \widetilde{\mathscr{E}}(t_k, u_h, z_h) - \rho(z_h, 1)$$

by using Algorithm 3.1, i.e., set $z_h^k = s_h^{stop}$ with s_h^{stop} computed by Algorithm 3.1.
(3) Stop if $k = N$. Otherwise, increase $k \to k+1$ and continue with (1).

The optimality condition for u_h^k in step (1) of the algorithm reads

$$\int_\Omega f(z_h^{k-1})e(u_h^k) : \mathbb{C}e(v_h)\,\mathrm{d}x = -\int_\Omega e(g(t_k)) : \mathbb{C}e(v_h)\,\mathrm{d}x + \int_{\Gamma_{\mathrm{Neu}}} u_{\mathrm{Neu}}(t_k)\cdot v_h\,\mathrm{d}s$$

for all $v_h \in \mathbf{U}_h$. In our computation we replace g by $g_h = \mathscr{I}_h g$ on the right-hand side with $\mathscr{I}_h$ being the nodal interpolant and g sufficiently smooth. We further use the midpoint rule to compute for $T \in \mathscr{T}_h$ and $e \in E_h$ the integrals

$$\int_T f(z_h^{k-1})\,\mathrm{d}x, \quad \text{and} \quad \int_e u_{\mathrm{Neu}}(t_k)\cdot v_h\,\mathrm{d}s.$$

The computation of u_h^k then amounts to solving a linear system of equations with a weighted stiffness matrix.

4 Existence result on a discrete level

In this section we show that suitable time-interpolants of the solutions $(u^k_{Nh}, z^k_{Nh})_{Nh}$ obtained at each time step t^k_N via the alternate minimization problem (5) satisfy a discrete version of the semistable energetic formulation (6). To this end, with $\mathscr{S}^1(\mathscr{T}_h)^d$ and $\mathscr{S}^1(\mathscr{T}_h)$ from (7), we set in (5)

$$\mathbf{U}_h := \mathscr{S}^1(\mathscr{T}_h)^d \cap \{v \in C(\overline{\Omega};\mathbb{R}^d), v = 0 \text{ on } \Gamma_D\} \text{ and } \mathbf{X}_h := \mathscr{S}^1(\mathscr{T}_h). \tag{14}$$

We recall that $\mathbf{U}_h \subset H^1_D(\Omega;\mathbb{R}^d)$ and $\mathbf{X}_h \subset BV(\Omega)$ for all $h > 0$ and

$$\bigcup_h \mathbf{U}_h \subset H^1_D(\Omega;\mathbb{R}^d) \text{ densely and } \bigcup_h \mathbf{X}_h \subset BV(\Omega) \text{ densely }. \tag{15}$$

We now choose a sequence $(h(N))_{N\in\mathbb{N}}$ such that $h(N) \to 0$ as $N \to \infty$ and consider a sequence of partitions $(\Pi_N)_N$ of $[0,\mathrm{T}]$ such that the time-step size $\Delta_N \to 0$ as $N \to \infty$. With $\mathscr{E}$ from (4) we introduce the energy functionals $\mathscr{E}_N : [0,\mathrm{T}] \times \mathbf{U} \times \mathbf{Z} \to \mathbb{R} \cup \{\infty\}$,

$$\mathscr{E}_N(t,u,z) := \begin{cases} \mathscr{E}(t,u,z) & \text{if } (u,z) \in \mathbf{U}_{h(N)} \times \mathbf{X}_{h(N)}, \\ \infty & \text{otherwise,} \end{cases} \tag{16}$$

where the given data $g(t)$ and $u_{\text{Neu}}(t)$ are replaced by suitably interpolated versions $g_N(t)$ and $u_{\text{Neu}N}(t)$ in the discrete spaces, which are uniformly bounded and converge strongly to the original datum. We thus compute for every $N \in \mathbb{N}$ and $h(N) > 0$, for each $t^k_N \in \Pi_N$ a solution $(u^k_N, z^k_N) = (u^k_{Nh(N)}, z^k_{Nh(N)})$ to (5) using Algorithm 3.2. In particular, according to Algorithm 3.1 the pair $(u^k_N, z^k_N) = (u^k_{Nh(N)}, z^k_{Nh(N)})$ satisfies

$$\forall u \in \mathbf{U}: \ \mathscr{E}_N(t^k_N, u^k_N, z^{k-1}_N) \le \mathscr{E}_N(t^k_N, u, z^{k-1}_N), \tag{17a}$$

$$\forall z \in \mathbf{X}:$$
$$\mathscr{E}_N(t^k_N, u^k_N, z^k_N) + \mathscr{R}(z^k_N - z^{k-1}_N) \le \mathscr{E}_N(t^k_N, u^k_N, z) + \mathscr{R}(z - z^{k-1}_N) + \mathrm{TOL}(N) \tag{17b}$$

with some $h(N)$-dependent tolerance $\mathrm{TOL}(N)$, which bounds the residual R^h_j, cf. Algorithm 3.1, Step (5). In view of Lemma 3.1 a sequence $(\mathrm{TOL}(N))_N$ can be chosen such that

$$\mathrm{TOL}(N)N \to 0 \text{ as } N \to \infty. \tag{18}$$

We evaluate the given data in the partition $\{t^0_N, \ldots, t^N_N\}$ which results in an $(N+1)$-tupel. Moreover, for any tupel $(v^0_N, \ldots, v^N_N)$ we introduce the piecewise constant left-continuous (right-continuous) interpolant $\overline{v}_N$ $(\underline{v}_N)$:

$$\overline{v}_N(t) := v^{k+1}_N \text{ for all } t \in (t^k_N, t^{k+1}_N], \tag{19a}$$

$$\underline{v}_N(t) := v^k_N \text{ for all } t \in [t^k_N, t^{k+1}_N). \tag{19b}$$

Accordingly, $\overline{\mathscr{E}}$, resp. $\underline{\mathscr{E}}$, indicates that the interpolants $\overline{g_N}$ and $\overline{u_{\text{Neu}}}_N$, resp. $\underline{g_N}$ and $\underline{u_{\text{Neu}}}_N$ are used. In particular, thanks to Assumptions 2.1 we have for all $t \in [0,\mathrm{T}]$

$$\overline{g}_N(t) \to g(t) \text{ in } \mathbf{U} \ \& \ \overline{u_{\text{Neu}}}_N(t) \to u_{\text{Neu}}(t) \text{ in } L^2(\Gamma_{\text{Neu}};\mathbb{R}^d). \tag{20}$$

This puts us in the position to find the following properties of the interpolants $(\overline{u}_N, \underline{u}_N, \overline{z}_N, \underline{z}_N)$ constructed from $(u^k_N, z^k_N)^N_{k=0}$ via (19):

Theorem 4.1 (Discrete version of (6) **and apriori estimates)** *Let the assumptions of Section 2 hold true and keep $N \in \mathbb{N}$ fixed. For each $k \in \{0,1,\dots,N\}$ let (u_N^k, z_N^k) satisfy* (17)*. Then the corresponding interpolants $(\overline{u}_N, \underline{u}_N, \overline{z}_N, \underline{z}_N)$ obtained via* (19)*, fulfill the following discrete version of* (6) *for all $t \in [0,\mathsf{T}]$:*

$$\text{for all } \tilde{u} \in \mathbf{U}: \quad \overline{\mathscr{E}}_N(t,\overline{u}_N(t),\underline{z}_N(t)) \le \overline{\mathscr{E}}_N(t,\tilde{u},\underline{z}_N(t)), \tag{21a}$$

$$\text{for all } \tilde{z} \in \mathbf{X}: \quad \overline{\mathscr{E}}_N(t,\overline{u}_N(t),\overline{z}_N(t)) \le \overline{\mathscr{E}}_N(t,\overline{u}_N(t),\tilde{z}) + \mathscr{R}(\tilde{z}-\overline{z}_N(t)) + \mathrm{TOL}(N), \tag{21b}$$

$$\overline{\mathscr{E}}_N(t,\overline{q}_N(t)) + \mathrm{Diss}_{\mathscr{R}}(\overline{z}_N,[0,t]) \le \overline{\mathscr{E}}_N(0,q_N^0) + \int_0^t \partial_\xi \mathscr{E}_N(\xi,\underline{q}_N(\xi))\,\mathrm{d}\xi + \mathrm{TOL}(N)N. \tag{21c}$$

In particular, there is a constant $C>0$ such that the following bounds hold true uniformly for all $N \in \mathbb{N}$:

$$\text{for all } t \in [0,\mathsf{T}]: \ \|u_N(t)\|_{\mathbf{U}} \le C, \tag{22a}$$

$$\text{for all } t \in [0,\mathsf{T}]: \ \|z_N(t)\|_{\mathbf{X}} + \|z_N(t)\|_{L^\infty(\Omega)} \le C, \tag{22b}$$

$$\mathscr{R}(\overline{z}_N(\mathsf{T}) - z_N^0) \le C \ \ \& \ \ \|\overline{z}_N\|_{BV(0,\mathsf{T};\mathbf{Z})} \le C, \tag{22c}$$

where (u_N, z_N) in (22a) *&* (22b) *stands for both $(\overline{u}_N, \overline{z}_N)$ and $(\underline{u}_N, \underline{z}_N)$.*

Proof 4.1 Proof of properties (21)**:** *Taking into account the definition* (19) *of the interpolants $(\overline{u}_N, \underline{u}_N, \overline{z}_N, \underline{z}_N)$ we see that minimality properties* (17) *can be directly translated into* (21a) *&* (21b)*. To find the discrete upper energy-dissipation estimate* (21c) *we test the minimality of u_N^k in* (17a) *by u_N^{k-1} and the minimality of z_N^k in* (17b) *by z_N^{k-1}. This results in*

$$\begin{aligned} \mathscr{E}_N(t_N^k, u_N^k, z_N^{k-1}) &\le \mathscr{E}_N(t_N^k, u_N^{k-1}, z_N^{k-1}) \\ \mathscr{E}_N(t_N^k, u_N^k, z_N^k) + \mathscr{R}(z_N^k - z_N^{k-1}) &\le \mathscr{E}_N(t_N^k, u_N^k, z_N^{k-1}) + \mathrm{TOL}(N). \end{aligned}$$

Let now $t \in (0, t_N^n]$ for some $n \le N$. Adding the above two inequalities, adding and subtracting $\mathscr{E}_N(t_N^{k-1}, u_N^{k-1}, z_N^{k-1})$, and summing over $k \in \{1,\dots,n\}$ we find

$$\begin{aligned} &\mathscr{E}_N(t_N^n, u_N^n, z_N^n) + \mathscr{R}(z_N^n - z_N^0) \\ &\le \mathscr{E}_N(t_N^0, u_N^0, z_N^0) + \sum_{k=1}^n \mathscr{E}_h(t_N^k, u_N^{k-1}, z_N^{k-1}) - \mathscr{E}_N(t_N^{k-1}, u_N^{k-1}, z_N^{k-1}) + n\mathrm{TOL}(N) \\ &= \mathscr{E}_N(t_N^0, u_N^0, z_N^0) + \sum_{k=1}^n \int_{t_N^{k-1}}^{t_N^k} \partial_\xi \mathscr{E}_N(\xi, u_N^{k-1}, z_N^{k-1})\,\mathrm{d}\xi + n\mathrm{TOL}(N), \end{aligned} \tag{23}$$

which yields (21c) *for all $t \in (0, t_N^n]$ and integers $n \le N$.*

Proof of estimates (22)**:** *Observe that there are constants $c_0, c_1 > 0$, such that for all $(t,u,z) \in [0,\mathsf{T}] \times \mathbf{U} \times \mathbf{Z}$ with $\mathscr{E}_N(t,u,z) < \infty$ it holds $|\partial_t \mathscr{E}_N(t,u,z)| \le c_1(c_0 + \mathscr{E}_N(t,u,z))$. This entitles us to apply a Gronwall estimate under the time-integral in* (23)*. Following the classical arguments for energy-dissipation inequalities in the rate-independent setting, cf., e.g., [43, Prop. 2.1.4], results in the estimates*

$$c_0 + \overline{\mathscr{E}}_N(t_N^k, u_N^k, z_N^k) \le (c_0 + \overline{\mathscr{E}}_N(0, u_N^0, z_N^0))\exp(c_1 T) \le C, \tag{24a}$$

$$\mathscr{R}(z_N^k - z_N^0) \le (c_0 + \overline{\mathscr{E}}_N(0, u_N^0, z_N^0))\exp(c_1 T) \le C, \tag{24b}$$

where the uniform boundedness by $C>0$ is due to (20) *and Assumption 2.1. The estimate* (22a) *is then standardly obtained from the bound* (24a)*, exploiting that $f(0) \ge a > 0$ and $\mu > 0$ by Assumption*

2.1, as well as Korn's and Young's inequality. The estimate (22b) *follows from the uniform boundedness of the damage gradients and the fact that* $I_{[0,1]}(z_N(t)) = 0$ *a.e. in* Ω*, ensured by* (24a)*, whereas the first estimate in* (22c) *is due to* (24b) *and the second is a direct consequence taking into account the form of* $\mathscr{R}$*, see* (1a)*. This concludes the proof of Prop. 4.1.* ■

5 Numerical Experiments

We report in this section the numerical results for two two-dimensional benchmark problems taken from [1] and [39].

5.1 Membrane with hole

In the sequel we specify all relevant information for the first benchmark problem from [1].

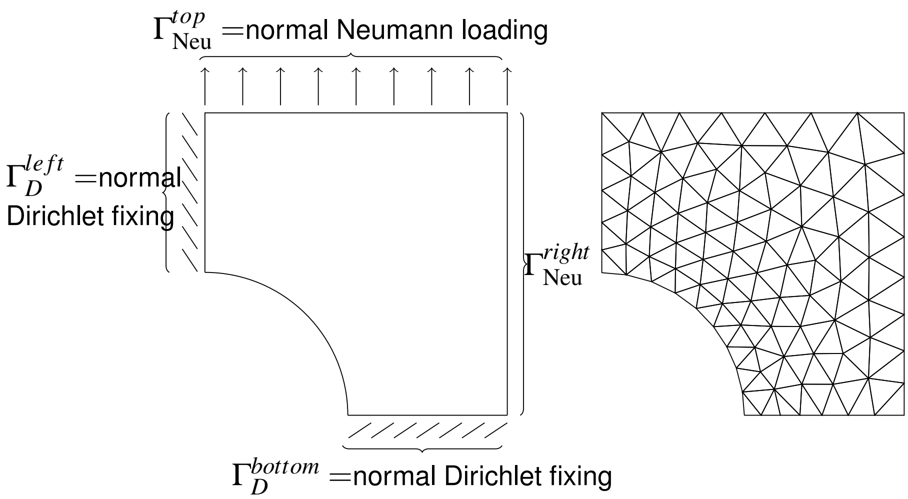

Figure 1: Left: Domain Ω and illustration of applied traction for membrane with hole: the material is pulled from above. Right: Coarse triangulation ($h_{\min} = 0.055$).

Problem specification:

We consider a body occupying a square domain with a hole around the center and which is pulled from above and below. Due to symmetry we regard only the upper right quarter of the domain. We summarize all relevant information for the first example in the following.

- **Geometry:** Length scale $L = 1$ mm;
  Domain $\Omega = (0,L)^2 \setminus \{x \in \mathbb{R}^2 : |x| \leq L\sqrt{2}/3\}$;
  Dirichlet boundary $\Gamma_D = ([L\sqrt{2}/3, L] \times \{0\}) \cup (\{0\} \times [L\sqrt{2}/3, L])$
- **Time horizon:** $\mathsf{T} = 1$ s

- **Load:** Dirichlet data:

$$u_D(t,x)_1 = 0\,\mathrm{mm/s} \quad \text{if } x \in \Gamma_D^{left},$$
$$u_D(t,x)_2 = 0\,\mathrm{mm/s} \quad \text{if } x \in \Gamma_D^{bottom};$$

Neumann data:

$$u_{\mathrm{Neu}}(t,x) = \begin{bmatrix} 0\,\frac{\mathrm{N}}{\mathrm{mm^2 s}} \\ t\cdot 1\,\frac{\mathrm{N}}{\mathrm{mm^2 s}} \end{bmatrix} \quad \text{if } x \in \Gamma_{\mathrm{Neu}}^{top},$$
$$u_{\mathrm{Neu}}(t,x) = \begin{bmatrix} 0\,\frac{\mathrm{N}}{\mathrm{mm^2 s}} \\ 0\,\frac{\mathrm{N}}{\mathrm{mm^2 s}} \end{bmatrix} \quad \text{if } x \in \Gamma_{\mathrm{Neu}}^{right};$$

The geometry and the applied traction are illustrated in Fig. 1.

- **Material parameters:** Young's modulus $E = 2900\,\mathrm{N/mm^2}$;
Poisson's ratio $\nu = 0.4$;
Lamé constants

$$\lambda = \frac{E\nu}{(1+\nu)(1-2\nu)} \approx 4142.9\,\frac{\mathrm{N}}{\mathrm{mm^2}},\ \mu = \frac{E}{2(1+\nu)} \approx 1035.7\,\frac{\mathrm{N}}{\mathrm{mm^2}};$$

The function f is chosen as $f(z) = a + (b-a)z$ with $a = 1/2$, $b = 1$;
Damage toughness $\rho = 4\cdot 10^{-4}\,\mathrm{N/mm^2}$;
Regularization factor $\kappa = 10^{-6}\,\mathrm{N/mm^2}$

- **Initialization:** Initial stable state $u_h^0 \equiv 0$, $z_h^0 \equiv 1$.

- **Discretization:** Four triangulations $\mathscr{T}_h$ generated with `distmesh` (see [46]) with mesh sizes (in mm)

$$h \approx 0.204,\ h_{\min} \approx 0.055; \quad h \approx 0.09,\ h_{\min} \approx 0.034;$$
$$h \approx 0.054,\ h_{\min} \approx 0.016; \quad h \approx 0.029,\ h_{\min} \approx 0.008;$$

Equidistant partition of $[0,\mathrm{T}]$ with $\Delta t = 10/(\lceil \mathrm{T}/h_{\min}^2 \rceil)$

- **Algorithm:** Algorithm 3.1 stops if $R_j \leq 10^{-6}/(2\max\{1, 1/(\tau_j h_{\min})\})$;
$\overline{\tau} = h_{\min}^{-2}$, $\underline{\tau} = 10^{-4}$, $\delta = 0.5$, $\underline{\gamma} = 0.5$, $\overline{\gamma} = 0.999$

Aim:

Since we are dealing with a BV-regularized damage model, i.e., the damage variable is allowed to jump in space, we want to investigate if the interfaces between damaged and undamaged parts of the material are sharp at least on the scale h of the mesh resolution. We will also compare the results with an H^1-regularization, i.e., we replace $\kappa|\mathrm{D}z|(\Omega)$ by $\kappa\|\nabla z\|^2$ and by $\kappa h_{\min}\|\nabla z\|^2$ in order to investigate the influence of the chosen regularization term on the damage evolution. The dependence of the solutions on the mesh size will also be analyzed.

Results:

DOI 10.20347/WIAS.PREPRINT.2388

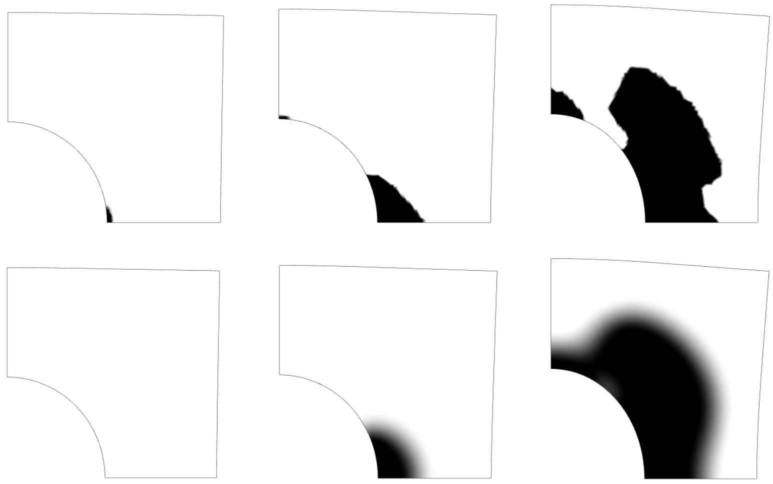

$t \approx 0.487$ $t \approx 0.723$ $t = 1$

Figure 2: Damage evolution with mesh size $h_{\min} \approx 0.008$ and time step size $\Delta t = 1/1492$. Top: BV-regularization. Bottom: Unweighted H^1-regularization. Displacements are magnified by factor 40.

$h_{\min} = 0.034$ $h_{\min} = 0.016$ $h_{\min} = 0.008$

Figure 3: Damage at $t = 1$ for different mesh sizes and time step sizes. Top: BV-regularization. Bottom: Weighted H^1-regularization with $\kappa h_{\min} \|\nabla z\|^2$. Displacements are magnified by factor 40.

In Fig. 2 three time steps of the damage evolution computed by Algorithm 3.2 for $h_{\min} = 0.008$ are depicted, both for the damage model with BV-regularization and unweighted H^1-regularization of the damage variable. The displacements are magnified by a factor of 40. One can clearly observe that the BV-regularization leads to sharp jumps (on the scale of h) while the transitions from undamaged ($z = 1$) to damaged ($z = 0$) parts of the material are smeared out for the H^1-regularization as it could be expected. The evolutions are more similar to each other if the H^1 regularization term is scaled with the factor $h_{\min}$ as it can be seen from Fig. 3. However, it is not clear whether the regularization term $\kappa h_{\min} \|\nabla z\|^2$ can be analytically justified, particularly with respect to the limit $h \to 0$.

In Fig. 4 we verify the energy estimate (21c) as a function of t_N^n, $n \leq N$, for three mesh sizes $h_{\min} = 0.055, 0.016, 0.008$. Obviously, the energy inequality holds and is increasing in time which is in accordance to (21c) since the inequality holds for all $t_N^k < t_N^n$, $1 \leq k \leq n \leq N$.

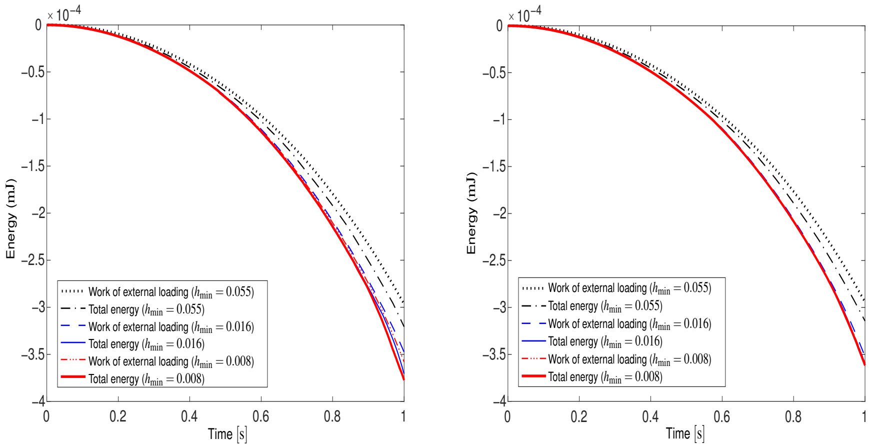

Figure 4: Verification of energy estimate (21c) as a function of t_N^n for three different mesh sizes. Sum of stored and dissipated energy ($=$ total energy $=$ left-hand side of (21c)); work of external loading up to time t_N^n ($=$ right-hand side of (21c) with $\overline{\mathscr{E}}_N(0,q_N^0) = 0$). Left: with BV-regularization; right: with H^1-regularization.

5.2 Notched square

The relevant information for the second test, which is taken from [39], are given below.

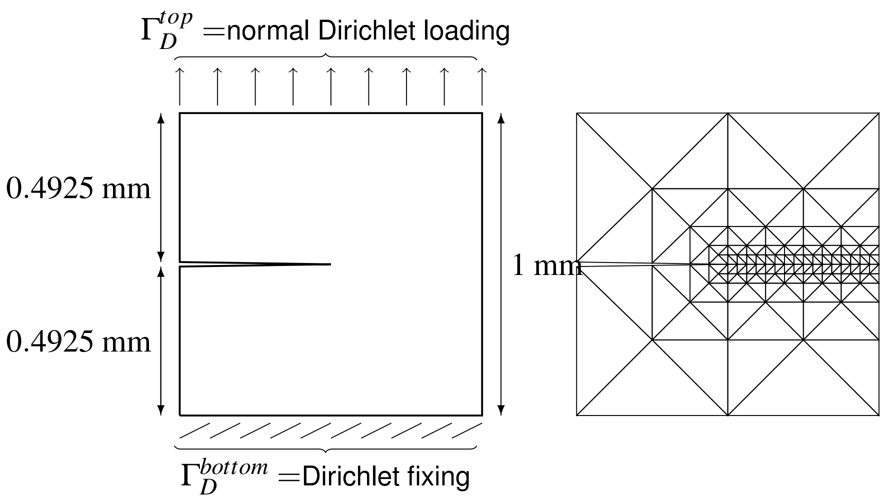

Figure 5: Left: Domain Ω and illustration of boundary conditions for notched square: the material is pulled from above. Right: Initial locally refined mesh.

Problem specification:

We consider a body occupying a square domain with a notch reaching from the middle of the left edge to the center of the specimen. The specimen is pulled from above and clamped at the bottom. We summarize all relevant information for this example in the following.

- **Geometry:** Length scale $L = 1$ mm;

Domain $\Omega = (0,L)^2 \setminus \mathrm{conv}\{(0,0.5075),(0.5,0.5),(0,0.4925)\}$;
Dirichlet boundary $\Gamma_D = ([0,L]\times\{0\})\cup([0,L]\times\{L\})$

- **Time horizon:** $\mathrm{T} = 1$ s
- **Load:** Dirichlet data:

$$u_D(t,x)_2 = t\cdot 0.002\,\mathrm{mm/s} \qquad \text{if } x\in\Gamma_D^{top},$$
$$u_D(t,x) = \begin{bmatrix} 0\,\mathrm{mm/s} \\ 0\,\mathrm{mm/s}\end{bmatrix} \qquad \text{if } x\in\Gamma_D^{bottom};$$

Neumann data:

$$u_{\mathrm{Neu}}(t,x) = \begin{bmatrix} 0\,\frac{\mathrm{N}}{\mathrm{mm}^2\mathrm{s}} \\ 0\,\frac{\mathrm{N}}{\mathrm{mm}^2\mathrm{s}}\end{bmatrix} \qquad \text{if } x\in\Gamma_{\mathrm{Neu}};$$

The geometry is illustrated in Fig. 5.

- **Material parameters:** Young's modulus $E = 210\,\mathrm{kN/mm^2}$;
  Poisson's ratio $\nu = 0.3$;
  Lamé constants

$$\lambda = \frac{E\nu}{(1+\nu)(1-2\nu)} \approx 121.15\,\frac{\mathrm{kN}}{\mathrm{mm}^2},\ \mu = \frac{E}{2(1+\nu)} \approx 80.77\,\frac{\mathrm{kN}}{\mathrm{mm}^2};$$

  The function f is chosen as $f(z) = a + (b-a)z$ with $a = 10^{-6}$, $b = 1$;
  Damage toughness $\rho = 2.7\cdot 10^{-3}\,\mathrm{kN/mm^2}$;
  Regularization factor $\kappa = 10^{-7}\,\mathrm{kN/mm^2}$

- **Initialization:** Initial stable state $u_h^0 \equiv 0$, $z_h^0 \equiv 1$.
- **Discretization:** Three triangulations $\mathscr{T}_h$ generated by uniform refinement of an initial mesh refined locally in region of expected damage evolution with mesh sizes (in mm)

$$h\approx 0.25,\ h_{\min}\approx 0.0156;\ h\approx 0.125,\ h_{\min}\approx 0.0078;\ h\approx 0.0625,\ h_{\min}\approx 0.0039;$$

  Equidistant partition of $[0,\mathrm{T}]$ with $\Delta t = 10/(\lceil \mathrm{T}/h_{\min}^2\rceil)$

- **Algorithm:** Algorithm 3.1 stops if $R_j \le 10^{-7}/(2\max\{1,1/(\tau_j h_{\min})\})$;
  $\overline{\tau} = h_{\min}^{-2}$, $\underline{\tau} = 10^{-3}$, $\delta = 0.5$, $\underline{\gamma} = 0.5$, $\overline{\gamma} = 0.999$

Aim:

The aim of this experiment is to compare the resulting damage evolution with established numerical experiments for damage or crack propagation reported in [39, 58], which are based on a phase field approach, and to check whether our damage model yields qualitatively the same results.

Results:

In Fig. 6 and 7 three snapshots of the damage evolution computed by Algorithm 3.2 for $h_{\min}\approx 0.0078$ are depicted for the damage model with BV-regularization and H^1-regularization, respectively, of the damage variable. Let us remark that the damage evolution observed in Fig. 6 qualitatively matches with the evolution reported in [39, Fig. 8] and [58, Fig. 4], i.e., the damage concentrates in a thin region around the horizontal line connecting the tip of the notch and the boundary on the right. Moreover, in contrast to the models discussed in [39, 58] the model presented in this paper is a damage model without phase field character and models by $a > 0$ only partial damage. Particularly, our model is not of Ambrosio-Tortorelli type.

In Fig. 8 the energy curves corresponding to (21c) as a function of t_N^n are depicted for three different mesh sizes . One can again observe that the energy inequality holds and that the gap is increasing in time. Furthermore, one can observe in Fig. 8 that the damage evolves relatively fast to the right boundary after the damage process has been initiated, e.g., for $h_{\min} = 0.0039$ it takes only a few milliseconds from initiation of the damage until damage reaches the boundary which is also in accordance with the observations made in [39, 58]. Note that the damage is triggered earlier for smaller mesh sizes which is on the one hand due to the singularity of the stress at the crack tip and on the other hand due to the finer partition of the time interval for smaller mesh sizes. This underlines the need for proper adaptive refinement techniques both for the space and the time variable.

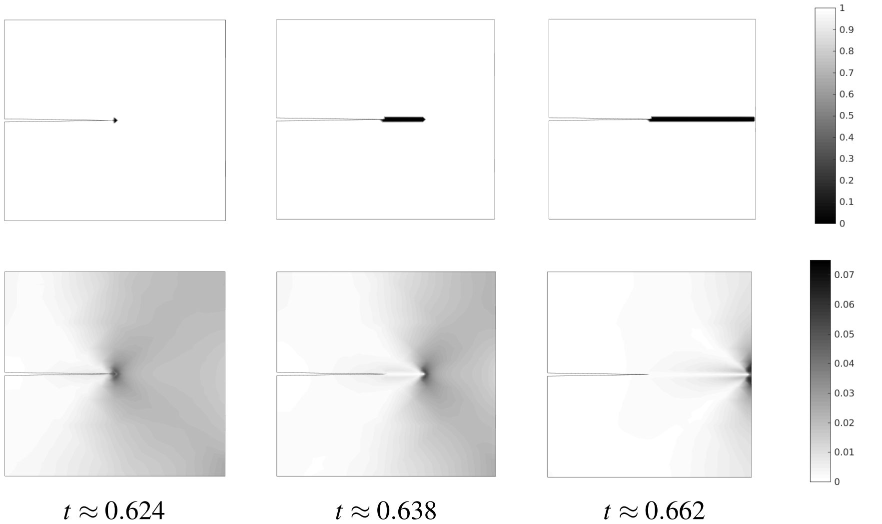

Figure 6: BV-regularized evolution for notched square with mesh size $h_{\min} \approx 0.0078$ and time step size $\Delta t = 1/1638$. Top: Evolution of damage variable z. Bottom: Stress $\sqrt{f(z)e(u+g(t)) : \mathbb{C}e(u+g(t))}$.

6 Conclusion

The numerical experiments show that our damage model can qualitatively capture the important features of damage evolution or crack propagation already reported in [39, 58, 10] for a phase field approach and, e.g., in [45, 51, 50] for similar numerical experiments based on energetic formulations. Depending on the particular setting the BV-regularization of the damage variable can lead to transitions from damaged to undamaged zones in the material that are significantly sharper than for an H^1-regularization as it has been observed in our first experiment.

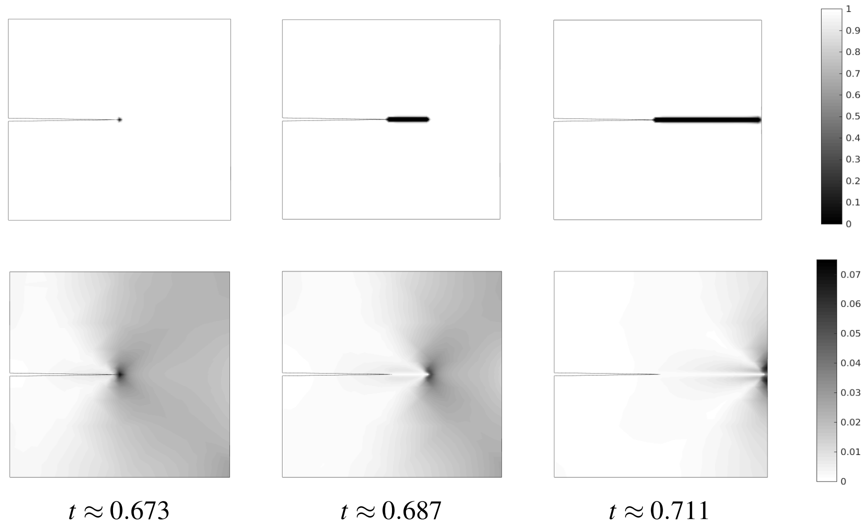

Figure 7: H^1-regularized evolution for notched square with mesh size $h_{\min} \approx 0.0078$ and time step size $\Delta t = 1/1638$. Top: Evolution of damage variable z. Bottom: Stress $\sqrt{f(z)e(u+g(t)):\mathbb{C}e(u+g(t))}$.

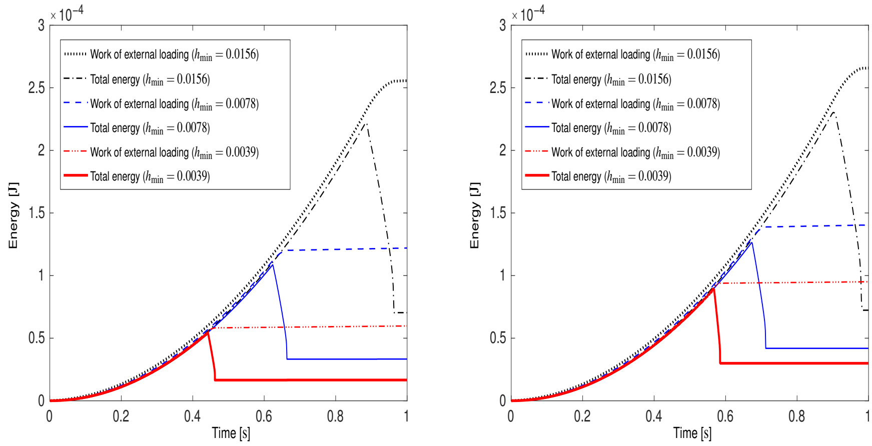

Figure 8: Verification of energy estimate (21c) as a function of t_N^n for three different mesh sizes. Sum of stored and dissipated energy (= total energy = left-hand side of (21c)); work of external loading up to time t_N^n (= right-hand side of (21c) with $\overline{\mathscr{E}}_N(0,q_N^0) = 0$). Left: with BV-regularization; right: with H^1-regularization.

Acknowledgments

This work was carried out within the project *Finite element approximation of functions of bounded variation and application to models of damage, fracture, and plasticity* within the DFG Priority Programme SPP 1748 “Reliable Simulation Techniques in Solid Mechanics. Development of Non-standard Discretisation Methods, Mechanical and Mathematical Analysis.”

References

[1] Alberty, J., Carstensen, C., Funken, S.A., Klose, R.: Matlab implementation of the finite element method in elasticity. Computing **69**, 239–263 (2002)

[2] Ambati, M., Kruse, R., De Lorenzis, L.: A phase-field model for ductile fracture at finite strains and its experimental verification. Comput. Mech. **57** (2016)

[3] Bartels, S.: Total variation minimization with finite elements: convergence and iterative solution. SIAM J. Numer. Anal. pp. 1162–1180 (2012)

[4] Bartels, S.: Numerical Methods for Nonlinear Partial Differential Equations. Springer, Heidelberg (2015)

[5] Bartels, S., Milicevic, M.: Alternating direction method of multipliers with variable step sizes (2017). URL https://aam.uni-freiburg.de/agba/prof/preprints/BarMil17-pre.pdf.Cited13Mar2017

[6] Beck, A., Teboulle, M.: Fast gradient-based algorithms for constrained total variation image denoising and deblurring problems. IEEE Transactions on Image Processing **18**, 2419–2434 (2009)

[7] Bonetti, E., Schimperna, G.: Local existence for Frémond's model of damage in elastic materials. Contin. Mech. Thermodyn. **16**(4), 319–335 (2004). DOI 10.1007/s00161-003-0152-2. URL http://dx.doi.org/10.1007/s00161-003-0152-2

[8] Bonetti, E., Schimperna, G., Segatti, A.: On a doubly nonlinear model for the evolution of damaging in viscoelastic materials. J. Differential Equations **218**(1), 91–116 (2005). DOI 10.1016/j.jde.2005.04.015. URL http://dx.doi.org/10.1016/j.jde.2005.04.015

[9] Bouchitté, G., Mielke, A., Roubíček, T.: A complete-damage problem at small strain. Zeit. angew. Math. Phys. **60**, 205–236 (2009)

[10] Bourdin, B.: Numerical implementation of the variational formulation for quasi-static brittle fracture. Interfaces and Free Boundaries **9**, 411–430 (2007)

[11] Braides, A., Cassano, B., Garroni, A., Sarrocco, D.: Quasi-static damage evolution and homogenization: a paradigmatic case of non-commutability. Ann. Inst. H. Poincaré Anal. Non Linéaire, online (2014)

[12] Brenner, S.C., Scott, L.R.: The Mathematical Theory of Finite Element Methods. Springer, New York (2008)

[13] Chambolle, A.: An algorithm for total variation minimization and applications. J. Math. Imaging Vis. **20**, 89–97 (2004)

[14] Chambolle, A., Pock, T.: A first-order primal-dual algorithm for convex problems with applications to imaging. J. Math. Imaging Vis. **40**, 120–145 (2011)

[15] Fiaschi, A., Knees, D., Stefanelli, U.: Young-measure quasi-static damage evolution. IMATI-Preprint 28PV10/26/0 (2010), Pavia (2010)

[16] Fortin, M., Glowinski, R.: Augmented Lagrangian Methods. North-Holland Publishing Co., Amsterdam (1983)

[17] Frémond, M.: Non-Smooth Thermomechanics. Springer-Verlag, Berlin (2002)

[18] Frémond, M., Nedjar, B.: Damage, gradient of damage and principle of virtual power. Internat. J. Solids Structures **33**, 1083–1103 (1996)

[19] Gabay, D., Mercier, B.: A dual algorithm for the solution of nonlinear variational problems via finite element approximation. Comp. & Maths. with Appls. **2**, 17–40 (1976)

[20] Glowinski, R.: Numerical Methods for Nonlinear Variational Problems. Springer, New York (1984)

[21] Glowinski, R., Le Tallec, P.: Augmented Lagrangians and Operator-Splitting Methods in Nonlinear Mechanics. IAM, Philadelphia (1989)

[22] Glowinski, R., Marroco, A.: Sur l'approximation par éléments finis d'ordre un, et la résolution, par pénalisation-dualité d'une classe de problèmes de dirichlet non linéaires. Revue française d'automatique, informatique, recherche opérationelle. Analyse numérique **9**, 41–76 (1975)

[23] Goldstein, T., O'Donoghue, B., Setzer, S., Baraniuk, R.: Fast alternating direction optimization methods. SIAM J. Imaging Sci. **7**, 1588–1623 (2014)

[24] Goldstein, T., Osher, S.: The split bregman method for l1 regularized problems. SIAM J. Imaging Sci. **2**, 323–343 (2009)

[25] Gurtin, M., Francis, E.: Simple rate-independent model for damage. Journal of Spacecraft and Rockets **18**(3), 285–286 (1981)

[26] Hackl, K., Stumpf, H.: Micromechanical concept for the analysis of damage evolution in thermo-viscoelastic and quasi-static brittle fracture. Int. J. Solids Structures **30**, 1567–1584 (2003)

[27] Halphen, B., Nguyen, Q.: Sur les matériaux standards généralisés. J. Mécanique **14**, 39–63 (1975)

[28] Hanke, H., Knees, D.: A phase-field damage model based on evolving microstructure, , vol. 101(3), pp. 149-180, 2017. Asymptotic Analysis **101**(3), 149–180 (2017)

[29] Heinemann, C., Kraus, C.: Existence of weak solutions for cahn–hilliard systems coupled with elasticity and damage. Adv. Math. Sci. Appl. pp. 321–359 (2011)

[30] Heinemann, C., Kraus, C.: Complete damage in linear elastic materials – modeling, weak formulation and existence results. Calc. Var. Partial Differ. Equ. pp. 217–250 (2015)

[31] Hintermüller, M., Rautenberg, C.N., Hahn, J.: Functional-analytic and numerical issues in splitting methods for total variation-based image reconstruction. Inverse Problems **30**(5), 055,014 (2014)

[32] Kachanov, L.: On creep rupture time (in russian). Izv. Acad. Nauk. SSSR, Otd. Techn. Nauk. (8), 26–31 (1958)

[33] Kachanov, L.: Introduction to Continuum Damage Mechanics, second edn. Mechanics of Elastic Stability. Kluwer Academic Publishers (1990)

[34] Knees, D., Negri, M.: Convergence of alternate minimization schemes for phase-field fracture and damage. accepted in M3AS (2015). URL `http://cvgmt.sns.it/media/doc/paper/2832/KneesNegri.pdf`

[35] Knees, D., Rossi, R., Zanini, C.: A vanishing viscosity approach to a rate-independent damage model. Math. Models Methods Appl. Sci. **23**(04), 565–616 (2013)

[36] Lions, P.L., Mercier, B.: Splitting algorithms for the sum of two nonlinear operators. SIAM J. Numer. Anal. **16**, 964–979 (1979)

[37] Marigo, J., Maurini, C., Pham, K.: An overview of the modelling of fracture by gradient damage models. Meccanica **51**(12), 3107–3128 (2016)

[38] Miehe, C., Hofacker, M., Welschinger, F.: A phase field model for rate-independent crack propagation: Robust algorithmic implementation based on operator splits. Computer Methods in Applied Mechanics and Engineering (2010)

[39] Miehe, C., Hofacker, M., Welschinger, F.: A phase field model for rate-independent crack propagation: robust algorithmic implementation based on operator splits. Computer Methods in Applied Mechanics and Engineering **199**, 2765–2778 (2010)

[40] Miehe, C., Welschinger, F., Hofacker, M.: Thermodynamically consistent phase-field models of fracture: Variational principles and multi-field FE implementations. Int. J. Numer. Meth. Engng. **83**, 1273âĂŞ1311 (2010)

[41] Mielke, A.: Evolution in rate-independent systems (Ch.6). In: C. Dafermos, E. Feireisl (eds.) Handbook of Differential Equations, Evolutionary Equations, vol. 2, pp. 461–559. Elsevier B.V., Amsterdam (2005)

[42] Mielke, A., Roubíček, T.: Rate-independent damage processes in nonlinear elasticity. Math. Models Methods Appl. Sci. **16**(2), 177–209 (2006)

[43] Mielke, A., Roubíček, T.: Rate-independent Systems: Theory and Application, *Applied Mathematical Sciences*, vol. 193. Springer (2015)

[44] Mielke, A., Roubíček, T., Zeman, J.: Complete damage in elastic and viscoelastic media and its energetics. Comput. Methods Appl. Mech. Engrg. **199**, 1242–1253 (2010). Submitted. WIAS preprint 1285

[45] Mielke, A., Roubíček, T., Zeman, J.: Complete damage in elastic and viscoelastic media and its energetics. Comput. Methods Appl. Mech. Engrg. **199**, 1242–1253 (2010)

[46] Persson, P.O., Strang, G.: A simple mesh generator in `matlab`. SIAM Review **42**, 329–345 (2004)

[47] Rocca, E., Rossi, R.: ”entropic” solutions to a thermodynamically consistent pde system for phase transitions and damage. SIAM J. Math. Anal. **74**, 2519–2586 (2015)

[48] Rockafellar, R.T.: Monotone operators and the proximal point algorithm. SIAM J. Control. Optim. **14**, 877–898 (1976)

[49] Roubíček, T., Thomas, M., Panagiotopoulos, C.: Stress-driven local-solution approach to quasistatic brittle delamination. Nonlinear Anal. Real World Appl. **22**, 645–663 (2015). DOI 10.1016/j.nonrwa.2014.09.011. URL `http://dx.doi.org/10.1016/j.nonrwa.2014.09.011`

[50] Roubíček, T., Panagiotopoulos, C.G., Mantič, V.: Local-solution approach to quasistatic rate-independent mixed-mode delamination (2015)

[51] Roubíček, T., Valdman, J.: Perfect plasticity with damage and healing at small strains, its modelling, analysis, and computer implementation. SIAM J. Appl. Math. **76**, 314–340 (2016)

[52] Rudin, L.I., Osher, S., Fatemi, E.: Nonlinear total variation based noise removal algorithms. Physica D **60**, 259–268 (1992)

[53] Schlüter, A., Willenbücher, A., Kuhn, C., Müller, R.: Phase field approximation of dynamic brittle fracture. Comput. Mech. **54**, 1141–1161 (2014)

[54] Thomas, M.: Quasistatic damage evolution with spatial bv-regularization. Discrete Contin. Dyn. Syst. Ser. S **6**, 235–255 (2013)

[55] Thomas, M., Bonetti, E., Rocca, E., Rossi, R.: A rate-independent gradient system in damage coupled with plasticity via structured strains. In: B. Düring, C.B. Schönlieb, M. Wolfram (eds.) Gradient flows: from theory to application, vol. 54, pp. 54–69. EDP Sciences

[56] Thomas, M., Mielke, A.: Damage of nonlinearly elastic materials at small strain: existence and regularity results. Zeit. angew. Math. Mech. **90**(2), 88–112 (2010)

[57] Weinberg, K., Dally, T., Schuß, S., Werner, M., Bilgen, C.: Modeling and numerical simulation of crack growth and damage with a phase field approach. GAMM-Mitt. **39**(1), 55–77 (2016)

[58] Weinberg, K., Dally, T., Schuß, S., Werner, M., Bilgen, C.: Modeling and numerical simulation of crack growth and damage with a phase field approach. GAMM-Mitt. **39**(1), 55–77 (2016)

[59] Wu, C., Tai, X.C.: Augmented lagrangian method, dual methods, and split bregman iteration for rof, vectorial tv, and higher order models. SIAM J. Imaging Sci. **3**, 300–339 (2010)